High-density Er-implanted GaN optical memory devices

Boon K. Lee, Robert Chih-Jen Chi, David Liang-Chiun Chao, Ji Cheng, Irving Yeong-Ning Chry, Fred R. Beyette, Jr., and Andrew J. Steckl

Upconversion emission has been obtained from Er-focused ion-beam (FIB) implanted GaN. Visible green emission at the 522- and 546-nm range were excited with infrared (IR) laser sources at either 840 or 1000 nm, or with both lasers simultaneously. By implanting closely spaced patterns with the FIB, we demonstrated the concept of storing data in Er-implanted GaN. Information stored as data bits consists of patterns of implanted locations as logic 1 and unimplanted locations as logic 0. The photon upconversion process in Er ions is utilized to read the stored information. This process makes use of the IR lasers to excite visible emission. The integrated upconversion emission power was measured to be ~40 pW when pumped by a 840-nm laser at 265 mW and by a 1000-nm laser at 208 mW. Patterns as small as 0.5 μm were implanted and read. Three-dimensional optical memory based on rare-earth-doped semiconductors could in theory approach a storage capacity of 10^{12} bits/cm^3.

OCIS codes: 210.0210, 160.5690, 210.4680, 230.4000, 260.3800.

1. Introduction

The increasing reliance of today's society on information services has fueled the ever-increasing demand for data storage. Current planar optical storage devices (such as CD-ROM, WORM, CD-R, CD-RW, MO, DVD) are insufficient to cope with the growing storage capacity requirements that are expected to exceed the terabyte per disk level[1] by the year 2010. Furthermore, with access speeds of the order of 10 Mbits/s, current systems cannot provide the data transfer rates necessary for practical utilization of terabyte storage systems. To satisfy the dual need for high density and fast access time, research in the area of optical data storage has begun focusing on alternative optical storage media. In contrast to current optical disk technologies that use far-field optics to read optically detectable data stored as a two-dimensional arrangement of bits, these alternative media are capable of exploiting either the increased resolution associated with near-field optics or the three-dimensional (3-D) potential of free-space optics.

With near-field technologies, such as a solid immersion lens, near-field scanning optical microscopy, and near-field arrays of vertical-cavity surface-emitting lasers, features as small as 10 nm in diameter can be read and written on an advanced optical disk.[2–5] The reduction in feature size has the potential to increase storage densities from 10^3 to 10^4 bits/μm^2. One drawback is that removable disks might not be possible. To achieve near-field resolution, the spacing between the optical disk and the read head is limited to the order of $\lambda/4$ or approximately 200 nm for near-IR operation. This extremely close proximity can be prohibitive for removable disk storage systems.

Alternatively, volumetric storage methods increase storage capacity by stacking data three dimensionally. Based on optical diffraction limitations, these 3-D optical memory systems have theoretical storage capacities approaching 10^{12} bits/cm^3. Furthermore, the incorporation of page-oriented preprocessing units designed to interface 3-D optical memories to existing electronic host systems should allow data transfer rates of the order of hundreds of megabits per second.[6,7] Thus archival storage systems based on 3-D optical memories should be capable of reasonable user access time while providing storage capacities significantly larger than the existing optical disk technologies.

First proposed in 1960, volumetric optical data

The authors are with the Nanoelectronics Laboratory, University of Cincinnati, 899 Rhodes Hall, P.O. Box 210030, Cincinnati, Ohio 45221-0030. The e-mail address for A. J. Steckl is a.steckl@uc.edu.

Received 19 September 2000; revised manuscript received 27 February 2001.
0003-6935/01/213552-07$15.00/0

storage has proven extremely difficult to achieve.[8–11] Currently, holographic data-storage,[12–14] multilayer disk technology,[15,16] and 3-D bit-oriented methods that use femtosecond lasers are the leading volumetric technologies.[17] All three approaches promise to provide storage density that is hundreds of times denser and access speeds that are faster than current optical disk media. However, they are not without technological barriers. Holography faces significant materials quality and stability issues. Absorption and multi-interface reflections may inhibit read and write operations to the lower layers of multilayer disks. Bit-oriented 3-D memories can require expensive lasers and optics and fail to provide high access speeds.

Rare earth- (RE-) doped integrated optical devices have recently generated a great deal of interest because of their broad applications in fiber lasers, fiber amplifiers, optical communications, optical sensing, high-resolution spectroscopy, and 3-D display.[18,19] A large variety of emission wavelengths are available, covering the UV, visible, and IR.[20–23] Furthermore, RE atoms emit light with a sharp linewidth associated with specific inner 4*f* shell transitions. It is therefore attractive to create a 3-D high-density, page-oriented memory device based on optical emission from RE-doped semiconductors. In fact, RE-based optical storage research has been gaining momentum with a variety of approaches, including spectral hole burning, photon echo, electron trapping, and even holography with a RE-doped storage medium.[24–27] However, these storage technologies have been limited by requirements for low-temperature operation, storage media that are difficult to manufacture, expensive broad-range tunable lasers, and concerns over scaling up from present bit-by-bit storage strategies. Therefore there is need for a simple method of implementing RE-based optical storage.

One approach for information to be stored is the implantion of a closely spaced pattern of single RE ions into an optically transparent wide bandgap semiconductor. Data bits would consist of a pattern of implanted locations as 1 and unimplanted locations as 0. This could be accomplished by focused ion-beam (FIB) implantation with spacing as small as 10–50 nm (depending on the species, energy, and substrate). In principle, this could result in an area bit density of from 10^{10} to 10^{12} bits/cm^2.

GaN is a III–V wide bandgap semiconductor material that has been shown[28,29] to be an excellent host for trivalent REs such as Er^{3+}, Pr^{3+}, Eu^{3+}, and Tm^{3+}. In the storage media the read operation could take advantage of the upconversion phenomenon in RE ions. Upconversion involves the absorption of two photons of the same or different energies producing the emission of a third photon of energy higher than that of either of the incident photons. We previously reported[30,31] green and red upconversion emission from Er and Pr ions FIB implanted into GaN. In this paper we utilize the upconversion effect in FIB Er-implanted GaN to evaluate its application to optical memory.

2. Experimental Conditions

To demonstrate the Er optical memory concept based on upconversion emission from FIB-implanted ions, closely spaced Er patterns (as small as 0.5 μm in size) were implanted by FIB into GaN films grown on sapphire and Si substrates. An Er–Ni liquid alloy ion source was fabricated to implant Er into GaN with a MicroBeam NanoFab-150 FIB system.[32] The Er^{2+} ion beam was accelerated to a 200-keV energy with doses ranging from 1×10^{12} to 1×10^{17} atoms/cm^2. GaN films used for Er incorporation were grown by molecular beam epitaxy (MBE), hydride vapor-phase epitaxy, and metal-organic chemical-vapor deposition. After implantation, samples were either annealed with rapid thermal annealing for 60 s or in a furnace at 1100 °C from 100 s to 1 h in nitrogen (N_2).

A schematic diagram of the experimental setup is shown in Fig. 1. We obtained upconversion spectra at room temperature by pumping the sample with two 500-mW cw tunable diode lasers, the SDL 8630 GaAs/AlGaAs at a 840-nm wavelength and the SDL TC30 InGaAs/AlGaAs at a 1000-nm wavelength. Both lasers were coupled into collinear beams and focused to a 2-μm-diameter beam spot through a modified Nikon Eclipse E600FN PhysioStation microscope with a Super Fluor 40×, 0.9-N.A. objective. The upconversion emission was collected through the same microscope objective. A dichroic mirror inside the microscope transmits at wavelengths below 800 nm and reflects both lasers and IR photoluminescence. The upconversion emission signal is fiber coupled to a 0.27-m Instrument S.A. 270M spectrometer equipped with a Spectrum One, 1024 × 256 pixel liquid-N_2-cooled Si CCD array detector. Spectra were acquired with SpectraMax software for spectrometer control and data acquisition. A grating of 300 grooves/mm blazed at a 500-nm wavelength was selected for spectrum collection.

A Melles-Griot NanoBlock *X–Y–Z* axis flexure stage with resolution up to a 20-nm step size was used for spatial scanning of the memory array. This translation stage provides both a 4-mm scanning range of fine position adjustment with 50-nm resolution along each axis and a high-resolution 20-μm scanning range at a 20-nm minimum step size by piezoelectric control drives. For added scanning range, the NanoBlock was placed on top of a Newport 401 two-axis large platform translation stage, which offers an additional 13-mm travel distance by two 860A-05 motorized drives. Computer automation for spatial scanning was written with LabVIEW programming software so that we could control both the spectrometer and the translation stages and construct spatial scanning profiles by integrating spectral intensity while simultaneously recording the scan position in real time. Three types of patterns were fabricated for spatial scanning detection: (a) square patterns with 136 μm × 136 μm and 50 μm ×

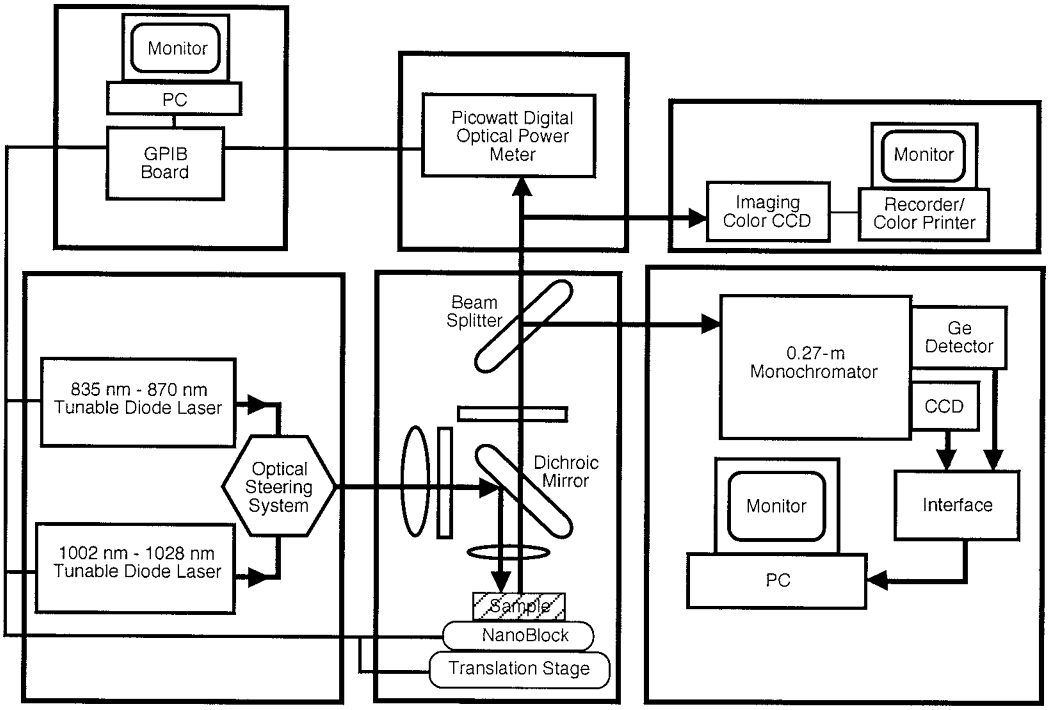

Fig. 1. Schematic diagram of optical characterization setup for upconversion optical memory storage based on Er-implanted GaN. GPIB, general-purpose interface bus.

50 μm dimensions; (b) rectangular patterns 20 μm in height with a variable width (0.5, 1.0, 2.0 μm) and spacing (5, 10, 15 μm); (c) 3 × 3 array patterns containing 2 μm × 3 μm rectangles with 7-μm spacing.

3. Results and Discussion

Thermal annealing is necessary to activate the upconversion process after FIB implantation. Green upconversion emission, pumped by either single lasers or by two collinear laser beams, was observed. Emission spectra of implanted GaN films grown by MBE, hydride vapor-phase epitaxy, and metal-organic chemical-vapor deposition under the same thermal annealing condition are identical.

Figure 2 shows the allowed energy levels of Er^{3+} ions and four possible upconversion processes, namely, Ia, Ib, IIa, IIb. Er^{3+} ions can be excited by (I) two photons of the same energy and (II) two photons of different energy. Upconversion processes of Ia and Ib require only a single laser source, whereas upconversion processes of IIa and IIb utilize two laser sources. In all four upconversion processes, the resulting emission at 522 nm is attributed to the radiative transition from the $^2H_{11/2}$ excited state to the $^4I_{15/2}$ ground state, whereas the 546-nm emission is due to the transition from $^4S_{3/2}$ to the ground state.

Type I upconversion consists of simple two-photon processes, which involve a single laser source. The upconversion process Ia, which uses 840-nm laser pumping, begins with Er^{3+} ions being excited from the ground state to the intermediate $^4I_{9/2}$ state and then to virtual states above the upper $^2H_{11/2}$ and $^4S_{3/2}$ states. In the upconversion process Ib, Er^{3+} ions are excited by 1000-nm photons to the $^4I_{11/2}$ intermediate excited state and then to upper excited states. Type II upconversion consists of the two-step, two-frequency upconversion process, wherein two lasers at different wavelengths are employed. In process IIa, Er^{3+} ions are excited by 840-nm photons from the ground state to the intermediate $^4I_{9/2}$ state, followed by excitation to the upper states by

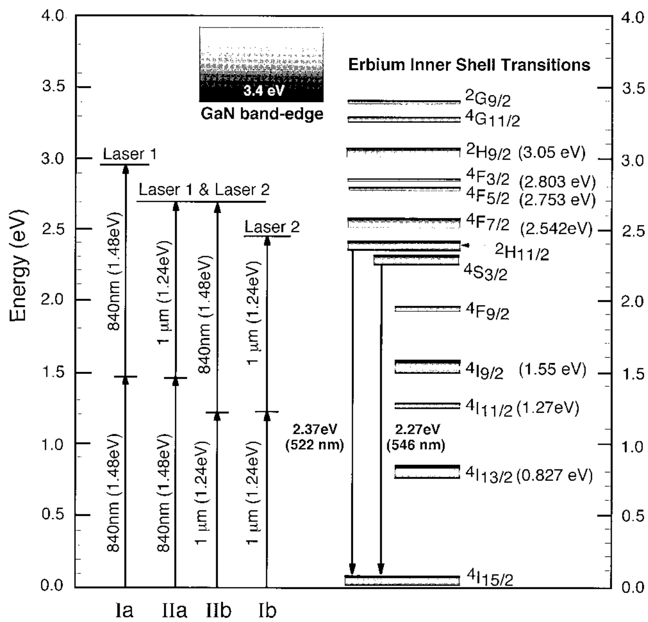

Fig. 2. Er energy levels and upconversion processes for FIB-implanted GaN:Er.

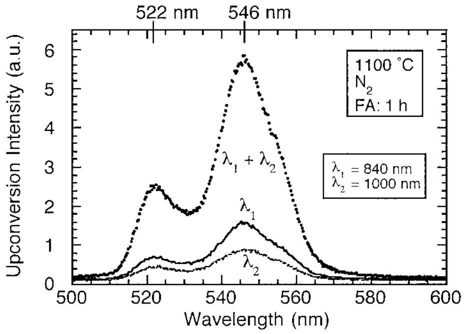

Fig. 3. Upconversion spectra under single and double laser pumping from FIB-implanted GaN:Er with 1-h furnace annealing (FA) at 1100 °C in N_2.

1000-nm photons. In process IIb the upconversion occurs in a reverse sequence. Er^{3+} ions are excited from the ground state to the intermediate $^4I_{11/2}$ state by 1000-nm photons, followed by excitation to the upper states by 840-nm photons. In all four processes, Er^{3+} ions, which are excited to the upper states, eventually relax to $^2H_{11/2}$ and $^4S_{3/2}$ states with nonradiative transitions. From these metastable states, excited ions gradually decay radiatively to the ground state with emission of green light.

Figure 3 contains typical upconversion spectra under single and double laser pumping from FIB Er-implanted GaN films grown on sapphire and annealed for 1 h at ~1100 °C. We implanted patterns on GaN films using a 200-keV Er^{2+} beam with a target current of 100 pA. The pixel exposure time was 0.46 ms, and the pixel size was 0.1 μm × 0.1 μm. This results in a dose of 1.4×10^{15} atoms/cm^2. Simulation of this condition by use of TRIM 95 calculates a projected range of ~38 nm and a peak concentration of ~3.7×10^{20} atoms/cm^3. All three spectra show peaks at 522 and 546 nm. We obtained the lowest intensity spectrum by pumping at 1000 nm. Use of the 840-nm laser increases the upconversion by a factor of 2. A 5× increase in upconversion intensity is generated when both lasers are used.

Figure 4 shows the upconversion intensity of FIB-implanted GaN films at 546 nm as a function of the Er-implanted dose from 4.3×10^{12} to 2.4×10^{16}/cm^2. After FIB implantation, samples were annealed at 1100 °C for 1 h in oxygen. The upconversion intensity was measured in the center of the pattern. The upconversion intensity at 546 nm becomes discernable for a dose of ~4×10^{12} atoms/cm^2 and increases up to a dose of ~10^{15} atoms/cm^2. A further increase in an Er dose results[30] in a decrease of the upconversion intensity. As suggested in Fig. 4, upconversion intensity dependence on an implanted Er dose can be used as a means to obtain gray-scale levels to increase storage capacity. In this case, four levels of intensity gray scale were demonstrated with 1 order-of-magnitude difference between each level.

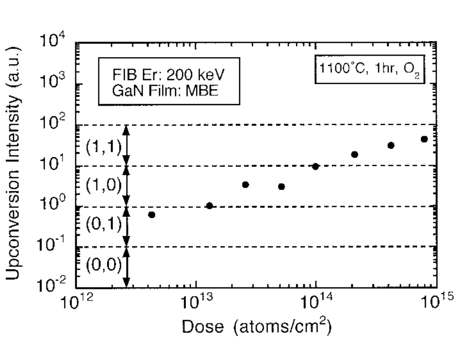

Fig. 4. Multiple-level storage capacity as a function of a FIB Er dose into GaN.

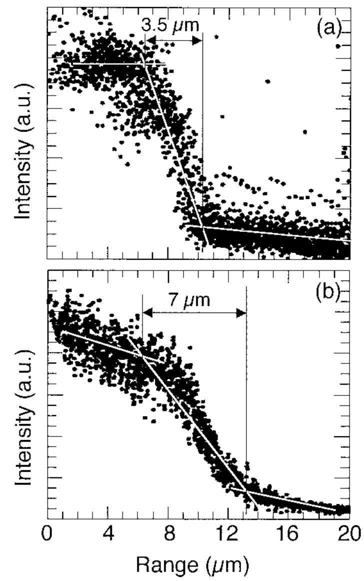

Fig. 5. Upconversion intensity across the edge of FIB-implanted GaN:Er samples. FIB dose is 10^{15}/cm^2. Furnace annealing at 1100 °C for a duration of (a) 100 s, (b) 1 h.

Upconversion intensity increases with annealing time for FIB-implanted GaN films. Although high upconversion intensity is a desired feature, there is an unintended issue. During annealing, thermal kinetic energy not only repairs the implantation damage, but also provides Er^{3+} ions with enough energy to diffuse away from the implanted area. Figure 5 shows this edge diffusion effect when the upconversion intensity is measured across the edge of regions implanted with a 10^{15}/cm^2 Er dose. The two Er-implanted GaN samples were furnace annealed at 1100 °C for 100 s and 1 h, respectively. The presence of nonzero photon counts in the unimplanted region is due primarily to stray light and noise picked up by the detection system. The transition region between the implanted and unimplanted areas is a function of annealing time, increasing from 3.5 μm for the 100-s anneal to 7 μm after the 1-h anneal. One must keep in mind that the laser beam diameter of ~2 μm determines the minimum measurable transition region width. Therefore the diffusion length for the 100-s annealing time is probably smaller than 3 μm.

The first optical memory was fabricated with a 3 × 3 array of FIB Er-implanted regions. Each bit has a nominal area of 2 μm × 3 μm with a center-to-center

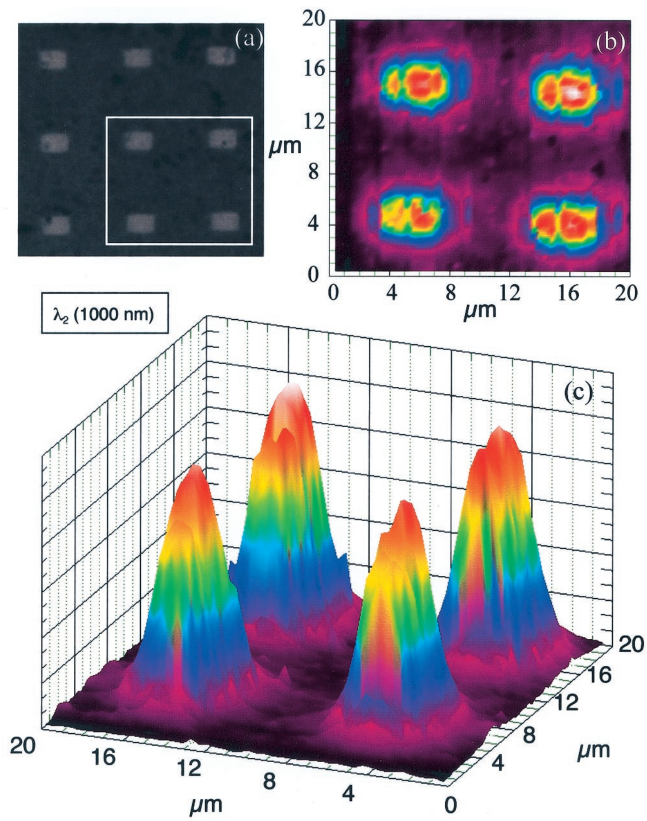

Fig. 6. Optical memory stored information in a FIB-implanted Er pattern: (a) reflected light image of a 3 × 3 array by optical microscopy; (b) upconversion image of 2 × 2 array, pumped with a 1000-nm laser; (c) scanned intensity profile of 2 × 2 array, pumped with a 1000-nm laser. The nominal bit area is 2 μm × 3 μm with a center-to-center spacing of 10 μm.

spacing of 10 μm. Er implantation conditions were 200-keV energy and a dose of 1×10^{15} atoms/cm^2. The GaN sample was rapid thermal annealed at 1100 °C for 60 s in N_2. Figure 6(a) shows the optical reflection image of the array. An upconversion image produced with a single pump laser at 1000 nm is shown in Fig. 6(b). We used LabVIEW programming software to automate both the spectrometer and the NanoBlock translation stage operation for obtaining high-resolution scanning profiles of the stored bits. The spectrum intensity integrated from 520 to 560 nm was recorded along with the scanning position to construct in real time the spatial scanning profile. A maximum 20 μm × 20 μm scanning sweep was performed with 400-nm steps. The collected data were transformed into a 3-D plot with HiQ software for better visualization. The scanned profile of a 2 × 2 subarray is shown in Fig. 6(c). The height of the plot corresponds to the integrated upconversion intensity. The spatial scanning profile of the bit area was measured to be slightly larger than the nominal implanted 2 μm × 3 μm. This is not unexpected when we take into consideration that the pump laser beam has a diameter larger than the implanted bit and that diffusion of the implanted Er occurs during annealing.

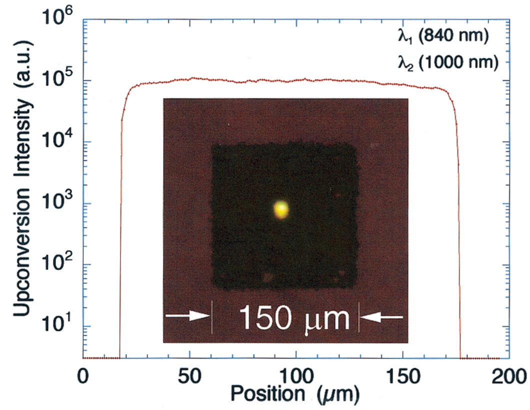

Fig. 7. Upconversion signal from a linear scan across a FIB-implanted GaN:Er region, pumped by both 840- and 1000-nm lasers.

Single upconversion scanning profiles across square and rectangular implanted patterns are shown in Figs. 7 and 8. These patterns were implanted with Er at 1×10^{15} atoms/cm^2 and furnace annealed at 1100 °C for 1 h. Collinear illumination was used to measure the spatial scanning profiles. Figure 7 shows the line scan across a 150 μm × 150 μm square pattern under dual-laser pumping. The difference in intensity between the implanted and the unimplanted area is approximately 3 orders-of-magnitudes higher than the intensity fluctuation at the implanted area. The width of the region over which diffusion has occurred at the edge of the pattern was measured to be ~10 μm.

To investigate the possibility of fabricating memory arrays with a higher bit density, we implanted and evaluated rectangular patterns with varying dimensions. Figure 8 shows a cross section and spatial scanning profile for three sets of three line patterns. Each set of line patterns consists of lines with a dimension of 2 μm × 20 μm on the left, 1 μm ×

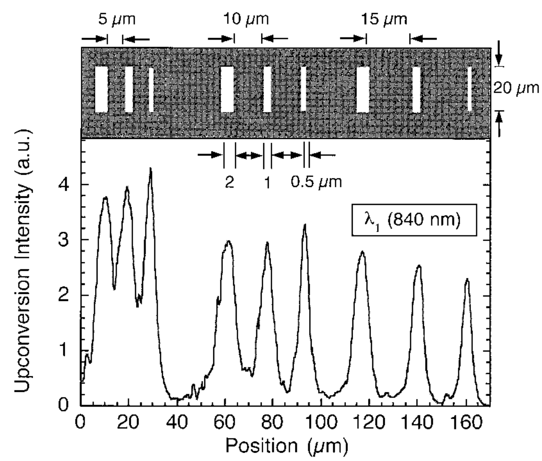

Fig. 8. Upconversion signal from a FIB Er-implanted rectangular pattern, pumped with a 840-nm laser. Each set contains rectangles with nominal values of a 2-, 1-, and 0.5-μm width at spacings of 5, 10, and 15 μm.

20 μm in the middle, and 0.5 μm × 20 μm on the right. The spacing between the lines in the line patterns is 5 μm wide for the lefthand set, 10 μm wide for the middle set, and 15 μm wide for the righthand set. As expected, the broadening caused by the 2-μm laser beam scan and the diffusion effect that is due to thermal annealing have made the measured linewidth slightly larger than the implanted size.

4. Summary and Conclusions

In summary we have demonstrated the concept of an Er-doped GaN optical memory device based on the upconversion process. Upconversion allows us to use commercially available IR semiconductor lasers to excite visible emission. Data, consisting of binary bit patterns, were recorded successfully by means of Er FIB implantation into GaN films grown on sapphire and Si substrates. The data can be read back sequentially through the detection of upconversion luminescence intensity. Bit patterns as small as 0.5 μm have been recorded and read successfully. This represents a bit density of $\sim 10^8$ bits/cm^2. An increase in bit density will require improvements in the writing process (reduction of FIB tails and edge diffusion of the implanted regions during anneal) as well as the reading technique (reduction in the beam diameters of the laser beams). Our research results show that the upconversion intensity can be controlled by the implanted Er dose. Four gray-scale levels for each written bit location have been demonstrated. Diffusion of the implanted species appears to limit the spacing between bits. We suspect that the diffusion effect is a result of the thermal process necessary for activation of the Gaussian FIB implantation profile. To resolve this problem, we propose to use a protective layer cap on top of GaN film prior to the implantation. This should allow us to obtain better control of the FIB profile and avoid the unwanted tail effect of the implantation.

In conclusion we have shown the feasibility of a high-density data-storage concept, which does not require sophisticated or radical storage system design. The current, conventional planar CD-ROM system format can be easily modified and integrated into our system. FIB is a well-developed technology, which has been widely applied in the semiconductor industry. Therefore, adapting FIB as means of a mass-production recording technique will allow us to use a dependable and proven technology. Although we have demonstrated a two-dimensional optical storage method, one could build a 3-D model by growing a multilayer GaN structure, with each layer written with FIB-implanted REs. This extension of our approach would result in an obvious increase of storage density ($\sim 10^{12}$ bits/cm^3) because of the more effective use of 3-D space. To read the data stored in such a 3-D optical memory, one could utilize the two-step, two-frequency upconversion process, which can be applied to Er excitation with two near-IR laser sources at 840 nm and 1.5 μm. Emission occurs only when two laser sources are coincident. By use of two orthogonal laser beams, individual locations within the 3-D structure can be read sequentially. In addition, because the upconversion intensity changes with an implanted RE dose, at least 2^2 gray-scale levels can be created for each written bit, further increasing the 3-D storage density available with this scheme. Finally, more than one RE species can be implanted into GaN films. For each additional i number of species used, a 2^i increase of storage states is possible.

This research has been supported in part by National Science Foundation grants ECS-9813588 and ECS-9906984. The authors acknowledge the support and encouragement of R. Khosla.

References

1. S. C. Esener, M. H. Kryder, W. D. Doyle, M. Keshner, M. Mansuripur, and D. A. Thompson, *The Future of Data Storage Technologies* (World Technology Division, International Technology Research Institute, Loyola College, Baltimore, Md., 1999), Chap. 1; http://itri.loyola.edu/hdmen/toc.htm.
2. E. Betzig, J. K. Trautman, R. Wolfe, E. M. Gyorgy, P. L. Finn, M. H. Kryder, and C.-H. Chang, "Near-field magneto-optics and high density data storage," Appl. Phys. Lett. **61,** 142–144 (1992).
3. B. D. Terris, H. J. Mamin, and D. Rugar, "Near-field optical data storage," Appl. Phys. Lett. **68,** 141–143 (1996).
4. S. M. Manfield and G. S. Kino, "Solid immersion microscope," Appl. Phys. Lett. **57,** 2615–2616 (1990).
5. K. Goto, "Proposal of ultrahigh density optical disk system using a vertical cavity surface emitting laser array," Jpn. J. Appl. Phys. **37,** 2274–2278 (1998).
6. M. E. Marhic, "Storage limit of two-photon-based three-dimensional memories with parallel access," Opt. Lett. **16,** 1272–1273 (1991).
7. S. Hunter, F. Kiamilev, S. Esener, D. A. Parthenopoulos, and P. M. Rentzepis, "Potentials of two-photon based 3-D optical memories for high performance computing," Appl. Opt. **29,** 2058–2066 (1990).
8. J. H. Strickler and W. W. Webb, "Three-dimensional optical data storage in refractive media by two-photon point excitation," Opt. Lett. **16,** 1780–1782 (1991).
9. D. Day and M. Gu, "Effects of refractive-index mismatch on three-dimensional optical data-storage density in a two-photon bleaching polymer," Appl. Opt. **37,** 6299–6304 (1998).
10. H. E. Pudavar, M. P. Joshi, and P. N. Prasad, "High-density three-dimensional optical data storage in a stacked compact disk format with two-photon writing and single photon readout," Appl. Phys. Lett. **74,** 1338–1340 (1999).
11. T. Nikolajsen, P. M. Johansen, X. Yue, D. Kip, and E. Kratzig, "Two-step two-color recording in a photorefractive praseodymium-doped La3Ga5SiO14 crystal," Appl. Phys. Lett. **74,** 4037–4039 (1999).
12. P. J. Van Heerden, "Theory of optical information storage in solids," Appl. Opt. **2,** 393–400 (1963).
13. G. T. Sincerbox, "Holographic storage—the quest for the ideal material continues," Opt. Mater. **4,** 370–375 (1995).
14. L. Hesselink, S. S. Orlov, A. Liu, A. Akella, D. Lande, and R. R. Neurgaonkar, "Photorefractive materials for nonvolatile volume holographic data storage," Science **282,** 1089–1094 (1998).
15. K. Baba, R. Yamada, S. Nakao, and M. Miyagi, "Three-dimensional optical disks using metallic island films: a proposal," Electron. Lett. **28,** 676–678 (1992).
16. J. R. Wullert II and P. J. Delfyett, "Multiwavelength, multilevel optical storage using dielectric mirrors," IEEE Photon. Technol. Lett. **6,** 1133–1135 (1994).

17. J. Qiu, K. Miura, H. Inouye, J. Nishii, and K. Hirao, "Three-dimensional optical storage inside a silica glass by using a focused femtosecond pulsed laser," Nucl. Instrum. Methods Phys. Res. B **141,** 699–703 (1998).
18. E. Downing, L. Hesselink, J. Ralston, and R. Macfarlane, "A three-color, solid-state, three-dimensional display," Science **273,** 1185–1189 (1996).
19. F. Goutaland, Y. Ouerdane, A. Boukenter, and G. Monnom, "Visible emission processes in heavily doped Er/Yb silica optical fibers," J. Alloys Compd. **275–277,** 276–278 (1998).
20. M. Dejneka, E. Snitzer, and R. E. Riman, "Blue, green and red fluorescence and energy transfer of Eu^{3+} in fluoride glasses," J. Lumin. **65,** 227–245 (1995).
21. J. M. Zavada and D. Zhang, "Luminescence properties of erbium in III-V compound semiconductors," Solid-State Electron. **38,** 1285–1293 (1995).
22. I. F. Elder and M. J. P. Payne, "Lasing in diode-pumped Tm: YAP, TM,Ho:YAP and Tm,Ho:YLF," Opt. Commun. **145,** 329–339 (1998).
23. E. B. Mejia, A. N. Starodumov, and Y. O. Barmenkov, "Blue and infrared up-conversion in $Tm3^{+}$-doped fluorozirconate fiber pumped at 1.06, 1.117, and 1.18 μm," Appl. Phys. Lett. **74,** 1540–1542 (1999).
24. S. Jutamulia, G. M. Storti, J. Lindmayer, and W. Seiderman, "Use of electron trapping materials in optical signal processing. 2: Two-dimensional associative memory," Appl. Opt. **30,** 2879–2884 (1991).
25. S. Kroll and P. Tidlund, "Recording density limit of photon-echo optical storage with high-speed writing and reading," Appl. Opt. **32,** 7233–7242 (1993).
26. E. S. Maniloff, S. B. Altner, S. Bernet, F. R. Graf, A. Renn, and U. P. Wild, "Recording of 6000 holograms by use of spectral hole burning," Appl. Opt. **34,** 4140–4148 (1995).
27. B. Plagemann, F. R. Graf, S. B. Altner, A. Renn, and U. P. Wild, "Exploring the limits of optical storage using persistent spectral hole-burning: holographic recording of 12000 images," Appl. Phys. B **66,** 67–74 (1998).
28. A. J. Steckl and J. M. Zavada, "Optoelectronic properties and applications of rare-earth-doped GaN," MRS Bull. **24**(9), 33–38 (1999).
29. A. J. Steckl, J. Heikenfeld, M. Garter, R. Birkhahn, and D. S. Lee, "Rare earth doped gallium nitride—light emission from ultraviolet to infrared," Compd. Semicond. **6,** 48–52 (2000).
30. L. C. Chao, B. K. Lee, C. J. Chi, J. Cheng, T. Chyr, and A. J. Steckl, "Upconversion luminescence of Er-implanted GaN films by FIB-direct write," Appl. Phys. Lett. **75,** 1833–1835 (1999).
31. L. C. Chao, B. K. Lee, C. J. Chi, J. Cheng, T. Chyr, and A. J. Steckl, "Rare earth FIB implantation utilizing Er and Pr liquid alloy ion sources," J. Vac. Sci. Technol. B **17,** 2791–2794 (1999).
32. L. C. Chao and A. J. Steckl, "Development of an Er-Ni liquid metal ion source," J. Vac. Sci. Technol. B **17,** 1051–1053 (1999).